



## INSPECTING THE NON DARCY FLOW OF VARIOUS SHAPED GRAPHENE OXIDE/ WATER NANOFLUID OVER POROUS EXPANDING DISK

**Arijit Mandal,**

Ph. D Scholar in Dr. A. P. J. Abdul Kalam University, Indore, Madhya Pradesh - 452016

E-mail: [arijitmandal.mld@gmail.com](mailto:arijitmandal.mld@gmail.com)

**Dr. Annapurna Ramakrishna Sinde,**

Department of Mathematics, Dr. A. P. J. Abdul Kalam University, Indore, Madhya Pradesh -  
452016

E-mail: [jayabhandari15@gmail.com](mailto:jayabhandari15@gmail.com)

**Dr. Md Tausif Sk,**

Department of Mathematics, Acharya B.N. Seal College, Cooch Behar - 736101, West  
Bengal, India

E-mail: [tausifdropbox@gmail.com](mailto:tausifdropbox@gmail.com)

**ABSTRACT:** MHD boundary layer flow of non Darcy nanofluid flow with various shapes like platelet, cylinder bricks and blade like shapes of Graphene Oxide (GO) with water as base fluid is taken into consideration. The nanofluid is flowing over a expanding disk which is permeable in nature. So suction and injection is also happening. An externally magnetic force field is applied in the flow system. Considering all those conditions we construct our flow model and with suitable transformations we transform the model into a dimensionless suit of ODEs with appropriate boundary conditions. Then with the help of a suitable numerical procedure, we produce the outcomes of the model and staged it through proper graphs and charts. Here we witnessed that nanoliquids with blade shaped nanoparticles has the best capacity to heat transfer. Also platelet shaped nanoparticles shows highest velocity and temperature in the study.

**KEYWORDS:** Non Darcy Flow; Expanding Disk; Various Shapes of Nanoparticle; External Magnetic Field; Suction/Injection; Graphene Oxide/ Water Nanofluid (GO/H<sub>2</sub>O) .

**2010 MATHEMATICS SUBJECT CLASSIFICATION:** 76W05

**DOI Number:** 10.48047/NQ.2022.20.20.NQ109308 **NeuroQuantology2022;20(20):3103-3118**

### 1. LITERATURE REVIEW:

Nanoliquid is the demand of current human civilization due to its usefulness in Biomedicine, Bioengineering, fuel extraction, nano chip production, heat transfer mechines, Geological survey, super computers, solar energy production, batteries production etc. Initially Choi [01] coined the concept of nanofluid which contains normal fluid with nano particles of metallic, non metallic materials in suspended form. This combination of liquid and solid increases the thermal intake capacity of the base fluid. That's why its been broadly used by researchers and scientists for further analysis and applications. Our aim in this article to cover the gap in theoretical knowledge about the nanofluids. There are many scholars who



were interested to find the correlation between thermophysical properties nanoparticles and liquids. Many were interested to analyze the important factors to influence the thermophysical properties of nanoliquids. Like Hamilton and Crosser [02] obtained the expression of thermal conductivity of nanoliquids considering the shape, component and compositions of the nanoparticles. Longman et al. [03] investigated unsteady nanofluid flow of  $Al_2O_3$ , Cu,  $TiO_2$  and Ag nanoparticles with the effect of thermal radiations. Then Aaiza et al. [04] analysed various shapes of nanoparticles in the energy flow in the mixed convection of nanoliquid flowing in porous medium. Khalid et al. [05] investigated five different types of nanoliquids flowing by free convection over a oscillating plate. Lately Hamid et al. [06] studied the stability of the flow of Graphene Oxide – Water nanofluid under the thermal radiation conditions.

For many decades the study of flow through porous medium is very much necessary due to its applications in ground water recovery, methen production from ground reservoirs, nuclear waste disposal, water purification process and many more. Initially Cheng and Minkowycz [07] analyzed the free convection in a vertical plate filled with porous medium. Then Hong et al. [08] inspected the non Darcy effect and nonuniform porosity effect on the natural convection of vertical porous medium. As per Darcy law the weight inclination is directly corresponding to the speed of the stream, which was set up tentatively by a one dimensional water move through stuffed sands at low speed. Be that as it may, the law is restricted in low speed stream and low Reynolds' number. Accordingly different endeavors were made by numerous researchers to vanish the impediment of the Darcy's law. In 1901, an Austrian architect P. Forchheimer made an improvement in Darcy's law by including a second request speed term to speak to the minute inertial impact because of the cooperation between solids and liquids in the stream and presented non-Darcy impact in the stream. Lai and Kulacki [09] studied non Darcy effect on the mixed convection in the varticle porous plate. Then Kandasamy et al. [10] evaluated the unsteady non Darcy flow of nanoliquid over a porous wedge. Recently, Sheikholeslami et al. [11] analyzed the entropy generation in the nanofluid flow with non Darcy effect in porous medium with magnetic force field. Ewis [12] considered a new approach to investigate MHD flow in non Darcy medium with hall corrent.

Many Biomedical engineering and mechanical engineering production requires to study the MHD flow over a rotating disk. Initially the flow over rotating disk is disigne by Von Karman [13]. After then various works had been done on this model. Like Millsaps and Pohlhausen [14] found exact solution of Von Karman flow of viscouse fluid in dimensionless form. Fang and Tao [15] worked on unsteady laminar flow over decelerating rotating disk and obtained numerical solution of two branches. Then Turkyilmazoglu and Uygun [16] analyzed compressible flow over rotating disk and solve it numerically to present the result numerically through graphs and charts. Miclavcic and Wang [17] incepted slip conditions on the viscous compressible flow over circulating disk. Similar study was done by Turkyilmazoglu [18] with the inception of Magnetohydrodynimcs. Then the effect of disk surface on the flow analysis was introduced by Turkyilmazoglu [19]. Then he [20] introduces

various nanoparticles in the nanofluid flow over the expanding disk. Griffiths [21] studied generalized Newtonian fluid flowing over a rotating disk and obtain the solution. Then extended the result to non Newtonian fluid like power law fluid and Carreau fluid. Doh and Muthamilselvan [22] investigated micropolar fluid flow over rotating disk. Tabassum and Mustafa [23] observed the Reiner–Rivlin fluid flow on a rotating disk. Then Appelquist et al. [24] inspected turbulent flow on the disk numerically. Butt and Ali [25] studied Entropy generation in Mhd nanofluid flow and investigated flow characteristics under various thermophysical assets of nanoparticles. Waini et al. [26] obtained the condition for dual solution existence in the MHD hybrid nanofluid flow over a rotating disk. Naqvi et al. [27] tried to find the importance of non uniform heat source and sink on the nanofluid flow on the expanding / contracting disk.

Our aim in this article is to find the effects of non Darcy factors, magnetic field and suction/injection on the porous disk which is linearly expanding. Also we tried to find the best shapes of Graphene Oxide nanoparticle for which the fluid performance in heat transfer is optimized.

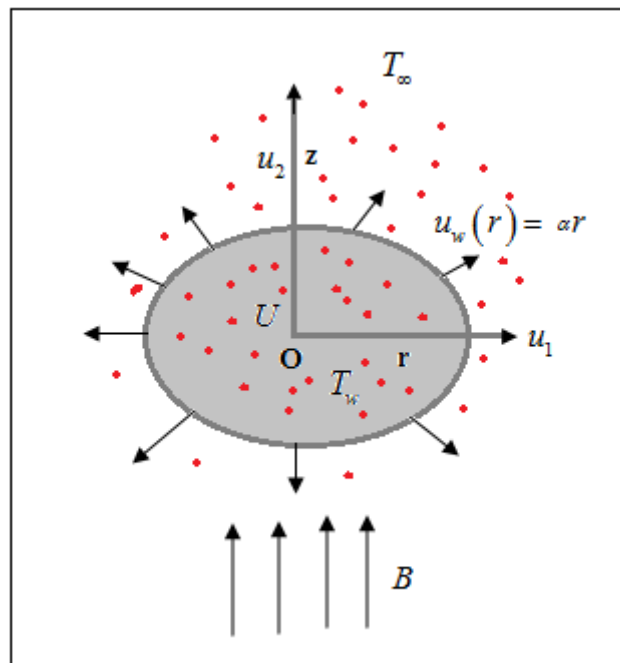


Figure 1: Physical flow model

## 2. PHYSICAL MODEL CONSTRUCTION:

To construct the required flow model we first need to consider incompressible viscous flow of thermally and electrically conducting flow of GO/water nanofluid over a radially expanding porous disk. An external magnetic field is applied to the flow as depicted in figure 1. The induced magnetic field is neglected. Considering the above facts [12,16] the mathematical model of the flow is as follows.

$$\left. \begin{aligned} \frac{\partial u_1}{\partial r} + \frac{u_2}{r} + \frac{\partial u_2}{\partial z} &= 0 \\ u_1 \frac{\partial u_1}{\partial r} + u_2 \frac{\partial u_1}{\partial z} &= \nu_{nf} \frac{\partial^2 u_1}{\partial z^2} - \frac{u_1}{\nu_{nf} K_1} - \frac{K_2}{\sqrt{K_1}} u_1^2 - \frac{\sigma B^2 u_1}{\rho_{nf}} \\ u_1 \frac{\partial T}{\partial r} + u_2 \frac{\partial T}{\partial z} &= \frac{\kappa_{nf}}{(\rho c_p)_{nf}} \frac{\partial^2 T}{\partial z^2} + \frac{\sigma B^2 u_1^2}{(\rho c_p)_{nf}} \end{aligned} \right\}$$

(1)

With suitable boundary conditions

$$\left. \begin{aligned} u_1 = \lambda u_w(r), u_2 = U, T = T_w \text{ at } z = 0 \\ u \rightarrow 0, T \rightarrow T_\infty \text{ as } z \rightarrow \infty \end{aligned} \right\}$$

(2)

Here  $(u_1, u_2)$  are the velocities of the flow in  $(r, z)$  direction,  $u_w(r) = \alpha r$  disk expanding speed,  $\lambda =$  expanding factor of the disk,  $U$  is mass flux velocity at the disk in  $z$  direction,  $T, T_w, T_\infty =$  temperatures of the fluid at any point, at wall of the disk, at far distance from the disk respectively,  $\nu = \mu/\rho$  kinematic viscosity,  $\mu =$  viscosity,  $\rho =$  density,  $K_1 =$  the porosity of the porous media i. e. drag of the flow introduced by Darcy,  $K_2 =$  Forchheimer inertia of the flow that ranges from 0.05 to 0.5 determined through experiments,  $\sigma =$  electrical conductivity of the fluid,  $B =$  transverse magnetic field,  $\kappa =$  thermal conductivity,  $c_p =$  specific heat capacity.

To make the equations (1-2) dimensionless and transform the set of PDEs into ODEs along with suitable boundary conditions, we introduce the following similarity transformations [16].

$$\left. \begin{aligned} u_1 = \alpha r g'(\xi), u_2 = -2(\alpha \nu_{bf})^{0.5} g(\xi), \theta = \frac{(T - T_\infty)}{(T_w - T_\infty)}, \xi = \left( \frac{\alpha}{\nu_{bf}} \right)^{0.5} z \end{aligned} \right\}$$

(3)

Applying the similarity transformations in equations (1) along with boundary conditions (2), the transformed suit of ODEs with suitable boundary conditions are given by

$$\left. \begin{aligned} \frac{\nu_{nf}}{\nu_{bf}} g''' + 2g g'' - \left( \frac{\nu_{bf}}{\nu_{nf}} k_1 + \frac{\rho_{bf}}{\rho_{nf}} M \right) g' - (k_2 + 1)(g')^2 &= 0 \\ \left( \frac{\kappa}{\rho c_p} \right)_{nf} \frac{1}{Pr} g'' + 2g g' + \frac{(\rho c_p)_{bf}}{(\rho c_p)_{nf}} EcM (g')^2 &= 0 \end{aligned} \right\}$$

(4)



$$\left. \begin{aligned} g = s, g' = \lambda, \mathcal{G} = 1 \text{ at } \xi = 0 \\ g' \rightarrow 0, \mathcal{G} \rightarrow 0 \text{ as } \xi \rightarrow \infty \end{aligned} \right\}$$

(5)

Here porosity factor  $k_1 = (\alpha v_{bf} K_1)^{-1}$ , coefficient of inertia  $k_2 = \frac{K_2 r}{\sqrt{K_1}}$ , magnetic factor  $M = \frac{\sigma B^2}{\alpha \rho_{bf}}$ , Prandtl Number  $Pr = \frac{v_{bf}}{\left(\frac{\kappa}{\rho c_p}\right)_{bf}}$ , Eckart number  $Ec = \frac{\alpha^2 r^2}{(c_p)_{bf} (T_w - T_\infty)}$ , suction /

injection factor  $s = \frac{-U}{2(\alpha v_{bf})^{0.5}}$ ,  $( )_X$  represents the properties of nanofluid, nanoparticles,

base fluids if  $X = nf, np, bf$  respectively.

Note: coefficient of inertia and Eckart numbers are depending on  $r$ . That implies the these two coefficients are locally similar. That's why we conclude that our results of the flow model are also locally similar.

The expression of nanofluid thermophysical properties like density [03], viscosity [04], thermal conductivity [02], specific heat intake capacity [05] is listed here.

$$\left. \begin{aligned} \rho_{nf} &= (1-\phi)\rho_{bf} + \phi\rho_{np} \\ \mu_{nf} &= \mu_{bf}(1+a\phi+b\phi^2) \\ \frac{\kappa_{nf}}{\kappa_{bf}} &= \frac{\kappa_{np} + (n-1)\kappa_{bf} + (n-1)(\kappa_{np} - \kappa_{bf})\phi}{\kappa_{np} + (n-1)\kappa_{bf} - (\kappa_{np} - \kappa_{bf})\phi} \\ (\rho c_p)_{nf} &= (1-\phi)(\rho c_p)_{bf} + \phi(\rho c_p)_{np} \end{aligned} \right\}$$

(6)

Here,  $a$  and  $b$  are the shapes of the nanoparticle depending constants,  $\phi$  is the nanoparticle volume fraction,  $n = \frac{3}{\psi^*}$  is the nanoparticle shape factor,  $\psi^*$  is the ratio of surface area

between the sphere and real nanoparticle of equal volume. The values of  $a, b$  and  $\psi^*$  are given in table 1. Also the values of thermo-physical properties of Graphene Oxide and water [06] are staged in Table 2.

Table 1: Values of  $a, b$  and  $\psi^*$

Shapes	Cylinder	Platelet	Brick	Blade
$a$	13.5	37.1	1.9	14.6
$b$	904.4	612.6	471.4	123.3
$\psi^*$	0.62	0.52	0.81	0.36

Table 2: Values of thermo-physical properties of GO & water

Thermo-physical assets	water	GO Nanoparticle
$\kappa$ (W/mk)	0.613	5000



$\mu$ (m.Pa.sec)	0.860420	---
$\rho$ (kg/m <sup>3</sup> )	997.1	1800
$c_p$ (J/g.K)	4.179	717

### 3. FLOW PERFORMANCE INDICATORS:

To define the flow performance we ought to observe the values of skin friction coefficient and Nusselt number. These coefficients can be determine by the following expressions

A. Skin friction coefficient:  $C_f = \frac{\tau_w}{\frac{1}{2}\rho_{nf}u_w^2}$ , here shear stress at the surface is

$\tau_w = \mu_{nf} \left( \frac{\partial u_1}{\partial z} \right)_{z=0}$ . Therefore the reduced skin friction is given by

$$Cf_r = \frac{1}{2} Re_r^{0.5} C_f = \frac{v_{nf}}{v_{bf}} g''(0).$$

B. Nusselt number of heat transfer:  $Nu = \frac{rq_w}{\kappa_{bf}(T_w - T_\infty)}$ , here thermal flux at the surface

is  $q_w = -\kappa_{nf} \left( \frac{\partial T}{\partial z} \right)_{z=0}$ . Therefore the reduced Nusselt number is

$$Nu_r = Re_r^{-0.5} Nu = -\frac{\kappa_{nf}}{\kappa_{bf}} g'(0).$$

Here  $Re_r = \frac{u_w(r)r}{v_{bf}}$  is local Reynold's number.

### 4. NUMERICAL PROCEDURE:

The suit of ODEs (4) and the reduced boundary conditions in (5) are being solved numerically due to its nonlinearity. For this reason we consider  $g = g_1, g' = g_2, g'' = g_3, g = g_4, g' = g_5$ . Considering those the transformed equations (4) takes the shape as

$$g_1' = g_2$$

$$g_2' = g_3$$

$$g_3' = \frac{v_{bf}}{v_{nf}} \left\{ -2g_1g_3 + \left( \frac{v_{bf}}{v_{nf}}k_1 + \frac{\rho_{bf}}{\rho_{nf}}M \right) g_2 + (k_2 + 1)(g_2)^2 \right\}$$

$$g_4' = g_5$$

$$g_5' = -Pr \frac{\left( \frac{\kappa}{\rho c_p} \right)_{bf}}{\left( \frac{\kappa}{\rho c_p} \right)_{nf}} \left\{ 2g_1g_5 + \frac{(\rho c_p)_{bf}}{(\rho c_p)_{nf}} EcM (g_2)^2 \right\}$$

The boundary conditions are  $g_1(0) = s, g_2(0) = \lambda, g_4(0) = 1$ . The above first order system of ODEs five variables to deduce. For that reason we need five initial conditions to solve it.

So we assume  $g_3(0) = \beta$  and  $g_5(0) = \delta$ . But in boundary conditions we get  $g_2(\infty) = 0$  and  $g_4(\infty) = 0$ . To solve the problem numerically we need to optimize the solution and obtain  $\beta$  and  $\delta$ . Then using Runge-Kutta Gill fourth order scheme we solve the IVP.

### 5. VALIDATION OF THE SOLUTIONS:

To check the validity of the result obtained by the above method, we first consider nanoparticle volume fraction  $\phi = 0$ ,  $s = 0$  and  $\lambda = 0$ . Then solve the first equation of (4) that transforms into  $g''' + 2gg'' - (g')^2 - Mg' = 0$  with boundary conditions  $g(0) = 0, g'(0) = 1$  and  $g'(\infty) = 0$ . We thus obtain the value of  $g''(0)$  for different values of  $M$  and compare the result with [25] in table 3. In the table 3 we witness an excellent degree of agreement.

Table 3: Comparison of values of  $g''(0)$

$M$	Butt and Ali [25]	Present paper
	$g''(0)$	$g''(0)$
0.0	-1.17372	-1.17372076083029
0.5	-1.36581	-1.36581450485325
1.0	-1.53571	-1.53571052855615
2.0	-1.83049	-1.83048967912036
3.0	-2.08484	-2.08484658214576

### 6. RESULT AND DELIBERATIONS:

After all those labourious work now we are able to unlock the influence of Darcy Forchheimer flow on the four distinct shapes of Graphne Oxide in GO / water nanofluid and also we staged the effects of presence of magnetic field, suction parameter and the stretching factor on the flow performance.

#### 6.1. Influence of permeability factor ( $k_1$ ) on the flow:

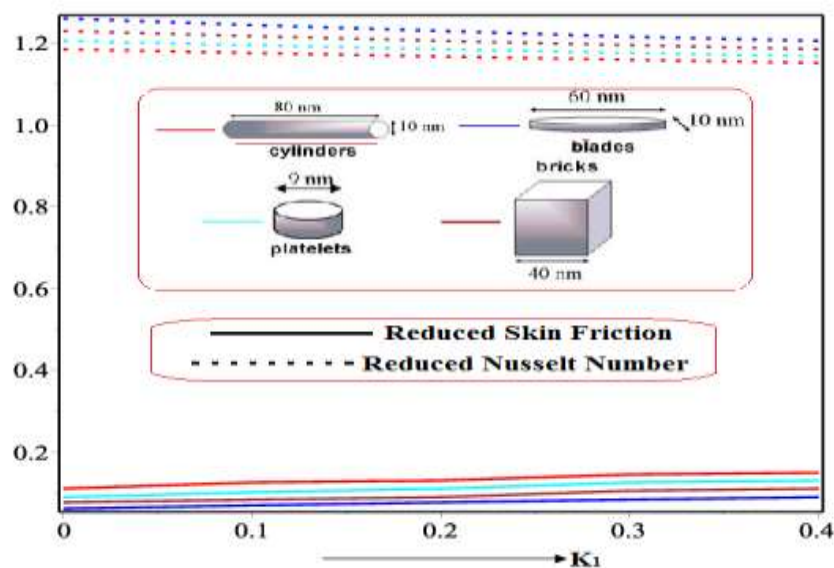


Figure 2: influence of  $k_1$  on physical measures

The effects of  $k_1$  on the flow performance is staged in figure 2-4. In figure 2, we depicted that with the raise in  $k_1$  the friction between flow surface and liquids elevates but heat transfer diminishes. Also among four different shapes of nanoparticles (NPs) blade shaped GO NPs shows highest capacity to transfer thermal energy and the least drag force at the wall. Permeability has the negative impact on the velocity of the flow as shown in figure 3. With the increment of porosity the velocity of the fluid diminishes. Also platelet shaped NPs has the highest velocity and blade shaped NPs has lowest velocity in the flow. Again we inspect that with the increment of porosity in the disk the difference between the velocity of four different NPs decreases. In case of temperature profile of the flow, the impact of porosity has positive effect on the flow as it increases the fluid temperature shown in figure 4. Here also platelet shaped NPs shows highest temperature followed by cylinder > bricks > blade.

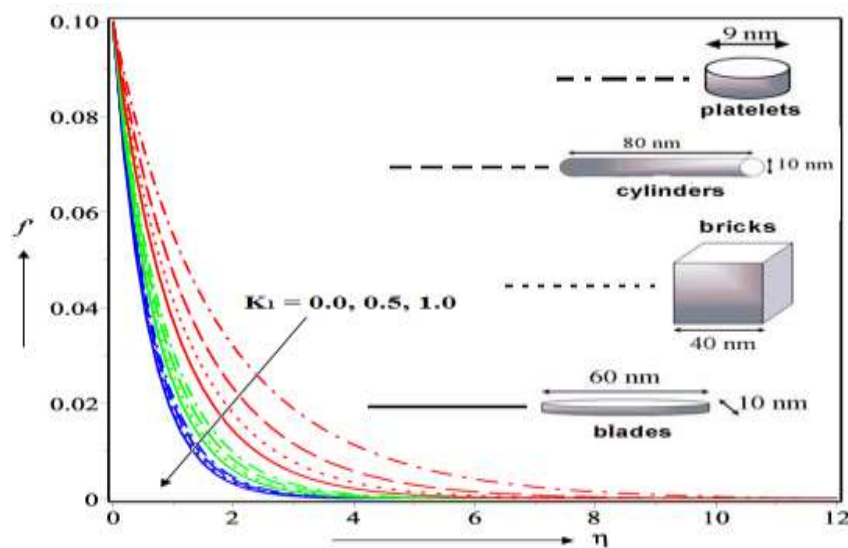


Figure 3: influence of  $k_1$  on velocity of the flow

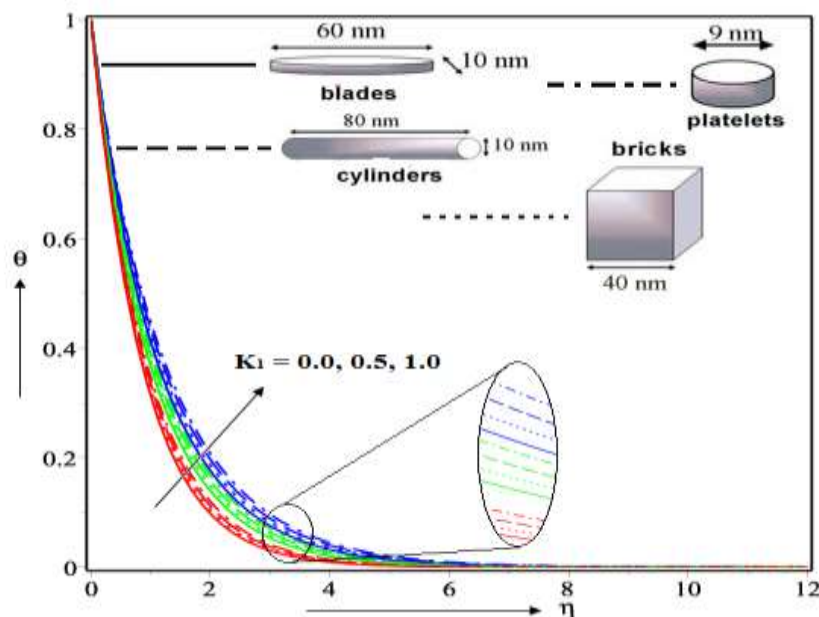


Figure 4: influence of  $k_1$  on temperature of the flow



### 6.2. Influence of Forchheimer factor ( $k_2$ ) on the flow:

The impact of  $k_2$  on the flow is staged in figure 5-7. The influence of  $k_2$  on the drag force between the solid surface and the liquids and the thermal flow of the fluid are not very significant as illustrated in figure 5. But in case of velocity it influenced quite remarkably staged in figure 6.  $k_2$  diminishes the fluid velocity continuously. But intensifies the temporal background of the flow with higher  $k_2$ .

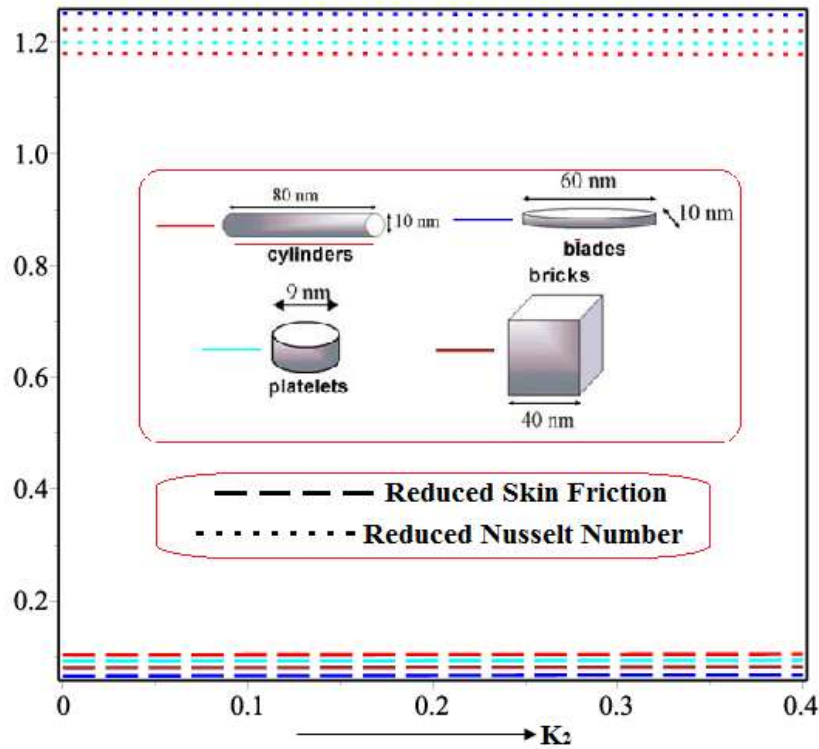


Figure 5: influence of  $k_2$  on physical measures

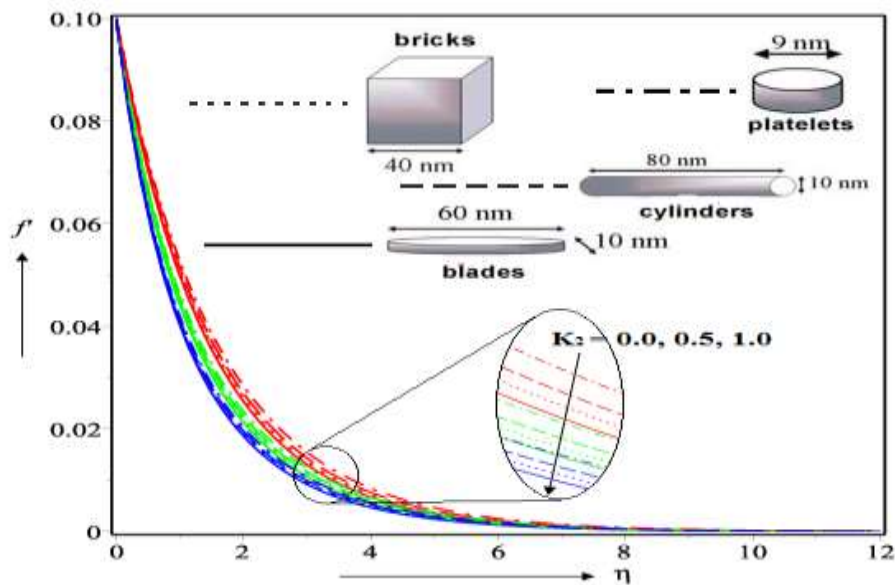


Figure 6: influence of  $k_2$  on velocity of the flow

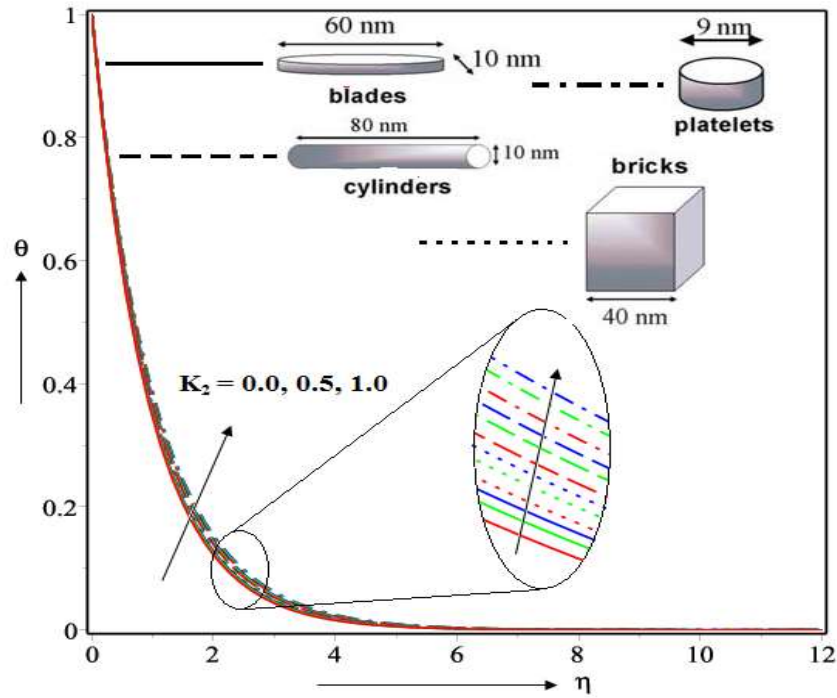


Figure 7: influence of  $k_2$  on temperature of the flow

### 6.3. Influence of magnetic force factor ( $M$ ) on the flow:

In figure 8-10, we tried to understand the effects of  $M$  on the fluid system. We observe in figure 8 that magnetic field intensifies the friction between flow surface and nanoliquids but reduces the thermal flow of the system staged in figure 8. Again in figure 9, we witness that presence of  $M$  demotivates the velocity of the flow. Also we observe that higher  $M$  lessens the gap of velocities of four distinct NPs. In figure 10, we inspect that  $M$  increases the temperature of the fluid in a continuous fashion.

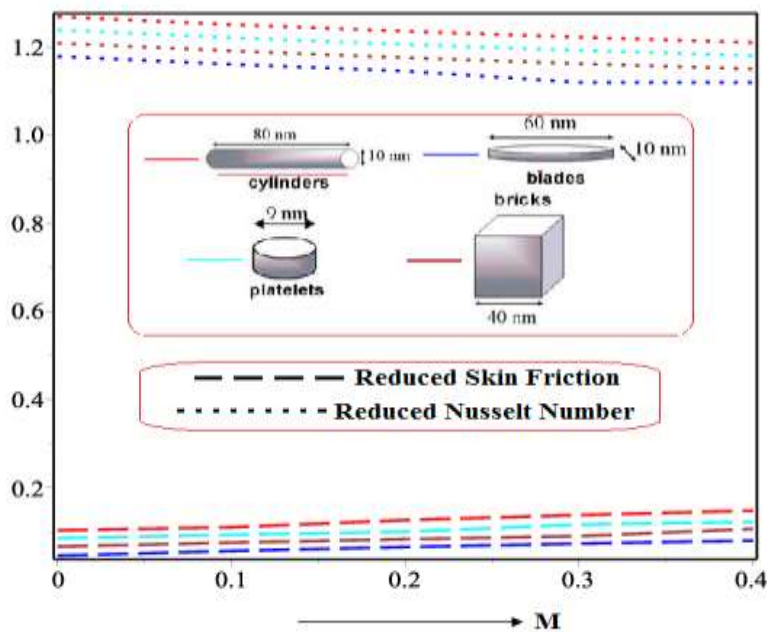


Figure 8: influence of  $M$  on physical measures

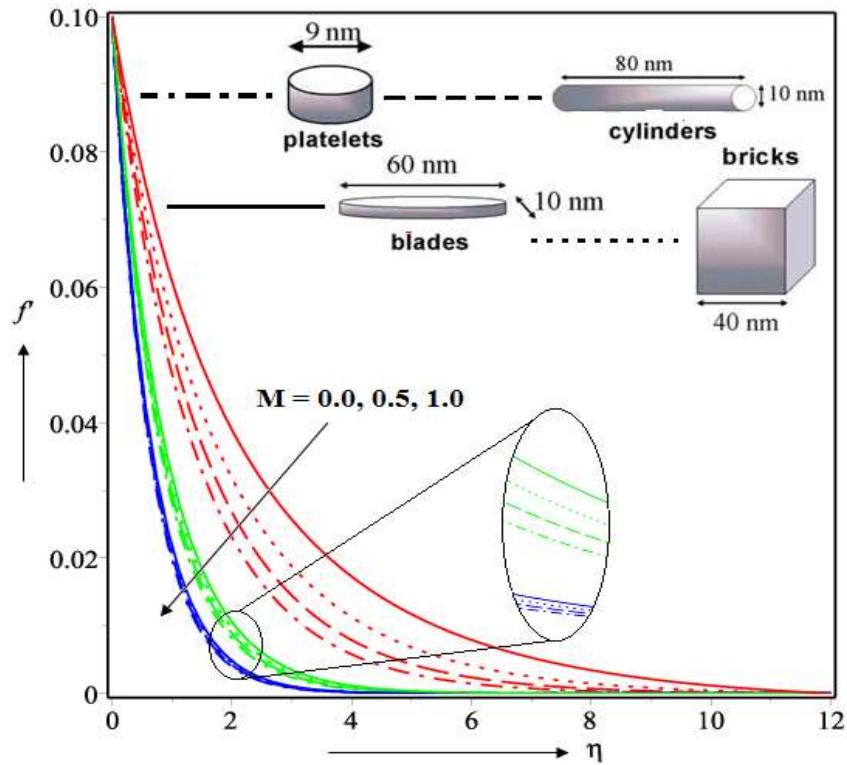


Figure 9: influence of  $M$  on velocity of the flow

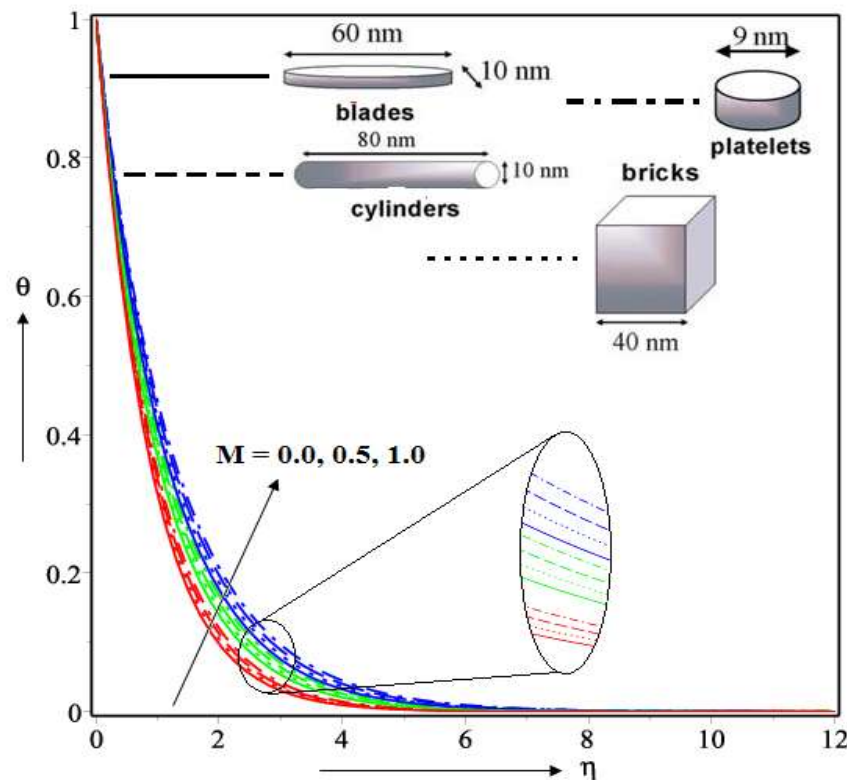


Figure 10: influence of  $M$  on temperature of the flow

#### 6.4. Influence of suction factor ( $s$ ) on the flow:

The influence of suction factor  $s$  is staged in figure 11-13. In figure 11 we observe that  $s$  has greatly impacted the thermal flow of the fluid but has negligible influence in skin friction. In

figure 12, we notice that higher  $s$  makes the flow slower. Similar case is shown in figure 13. We witness that suction lessens the thermal outcome of the fluid. But it is worthy to note that impact of  $s$  on velocity is less visible than effect on the temperature between four shapes of NPs.

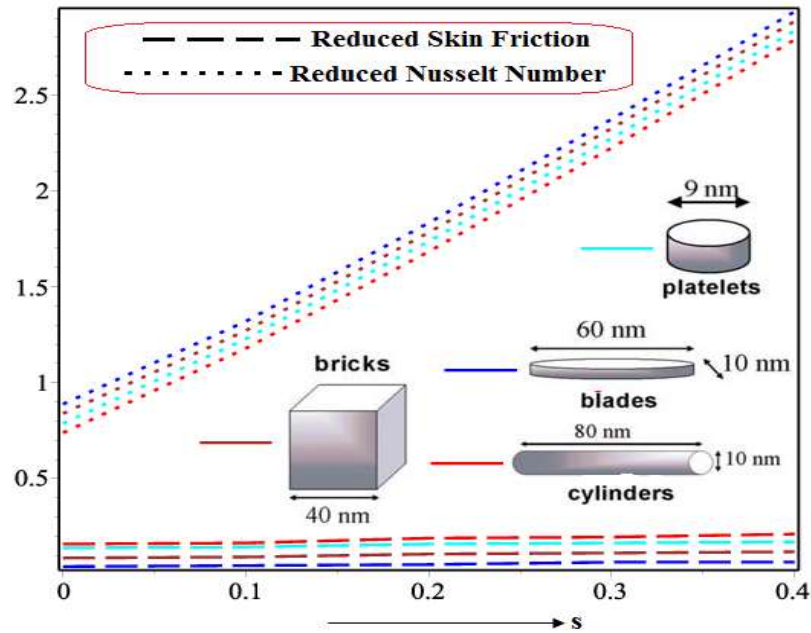


Figure 11: influence of  $s$  on physical measures

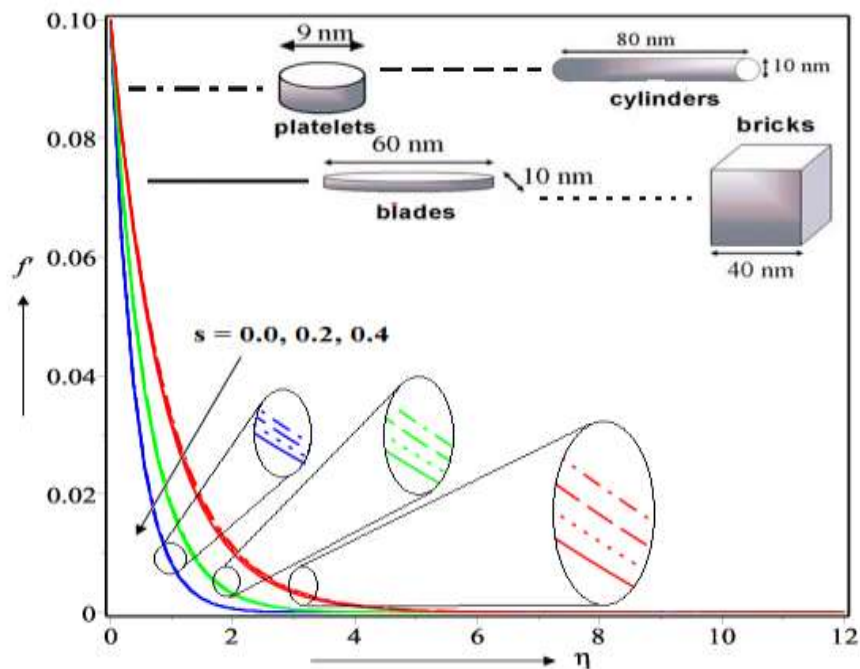


Figure 12: influence of  $s$  on velocity of the flow

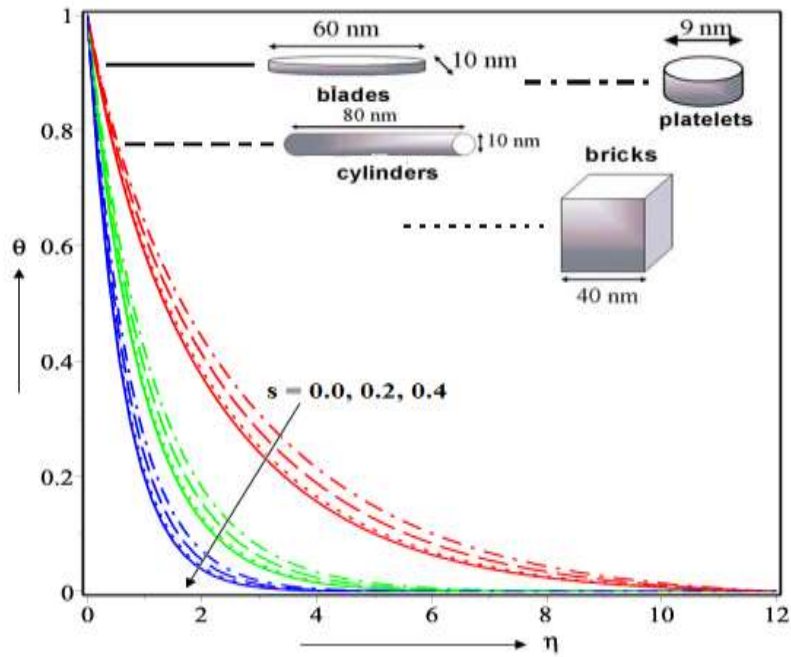


Figure 13: influence of  $s$  on temperature of the flow

### 6.5. Influence of expanding factor ( $\lambda$ ) on the flow:

At last the influence of the disk stretching factor  $\lambda$  on the flow is staged in figure 14-16. In figure 14 we notice that expanding factor  $\lambda$  amplifies both skin friction and thermal flow. Also in figure 15, it is analysed that higher  $\lambda$  intensifies velocity of the fluid. But in figure 16, we notice that higher  $\lambda$  diminishes the temperature of the of the fluid.

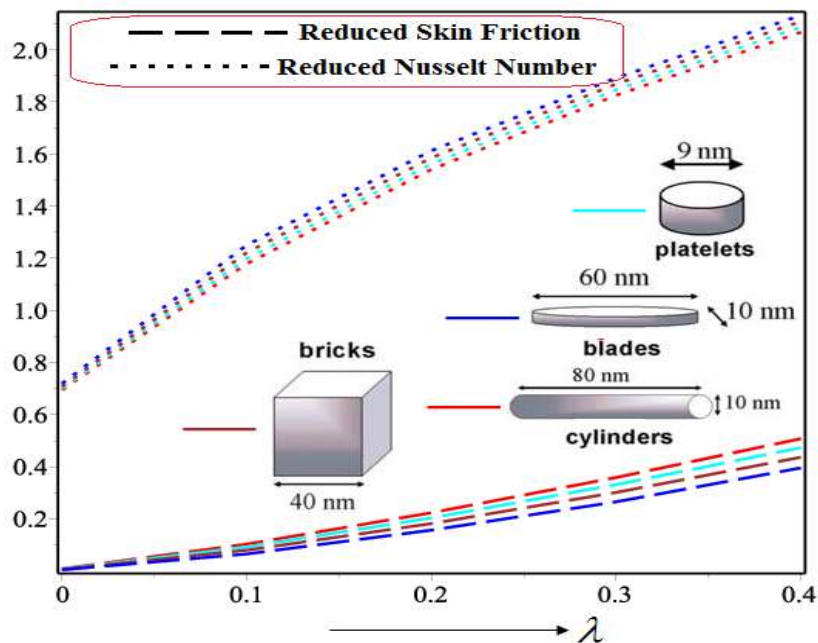


Figure 14: influence of  $\lambda$  on physical measures

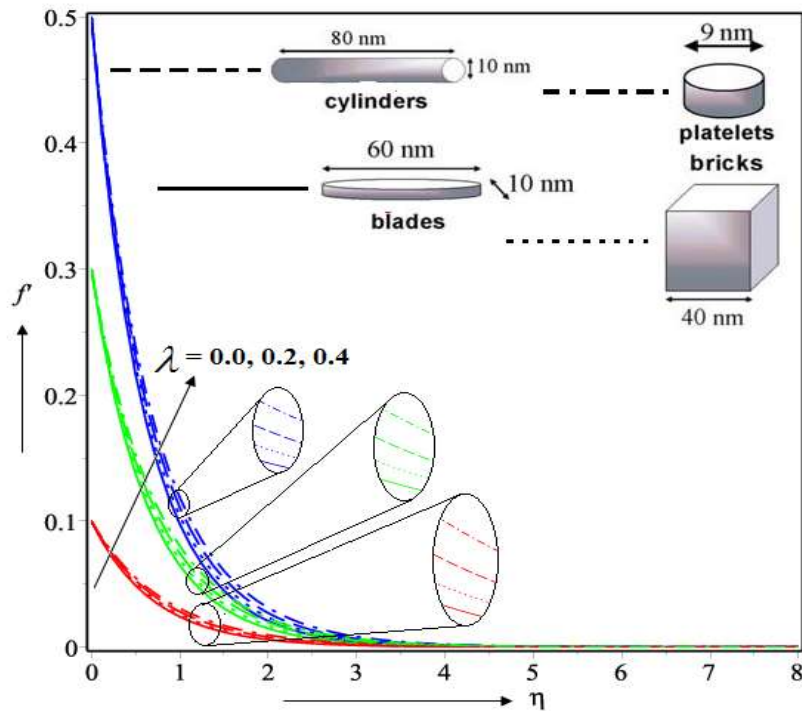


Figure 15: influence of  $\lambda$  on velocity of the flow

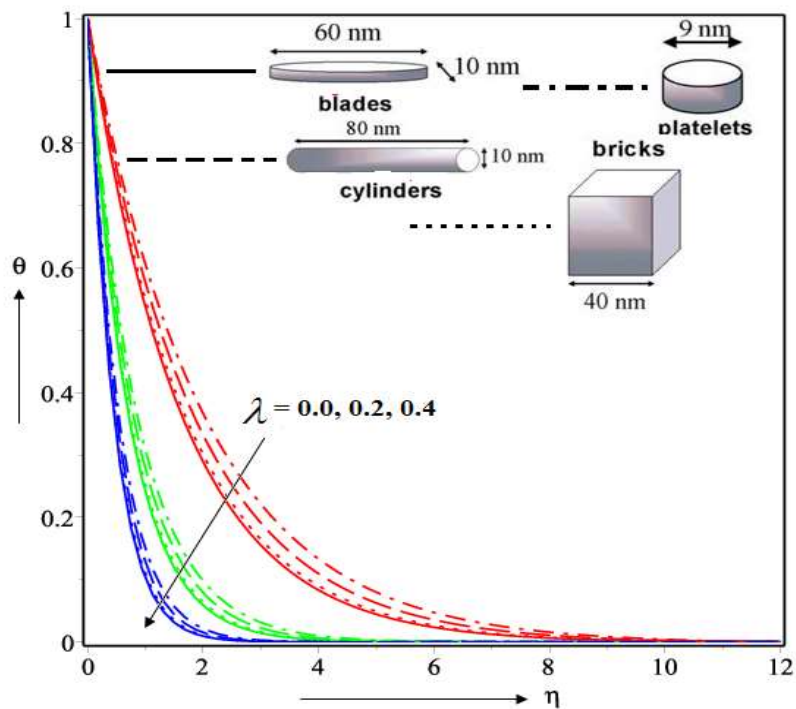


Figure 16: influence of  $\lambda$  on temperature of the flow

## 7. CONCLUSIONS:

In this article we analyzed Darcy Forchheimer flow of Graphene Oxide / water nanofluids over an expanding disk with different shapes of nanoparticles. An external transverse magnetic force field applied in z direction. The disk is treated as permeable surface. After construction and solving the model we come to some important conclusions about the flow which are listed below.

- Porosity factor influences skin friction and diminishes heat transfer.
- The expanding factor intensifies heat transfer the most in the flow.
- Blade shaped NPs shows the highest capacity to flow the thermal energies and lowest skin friction.
- Platelet NPs shows the highest velocities in the flow followed by cylinder > bricks > blades.
- Similar order is observed in case of temperature of the flow.
- To regulate the temperature of the fluid expanding factor and suction factors are the best candidate factor to control.
- Also to control the velocities of the fluid, expanding factor and suction factors are the most suitable regulators.

#### REFERENCES:

- [01] S. Choi, Enhancing thermal conductivity of fluids with nanoparticles, ASME Publ. Fed., 231, 1995, 99-106.
- [02] Hamilton, R.L. and Crosser, O.K., 1962. Thermal conductivity of heterogeneous two-component systems. *Industrial & Engineering chemistry fundamentals*, 1(3), pp.187-191.
- [03] Loganathan, P., Nirmal Chand, P. and Ganesan, P., 2013. Radiation effects on an unsteady natural convective flow of a nanofluid past an infinite vertical plate. *Nano*, 8(01), p.1350001.
- [04] Aaiza, G., Khan, I. and Shafie, S., 2015. Energy transfer in mixed convection MHD flow of nanofluid containing different shapes of nanoparticles in a channel filled with saturated porous medium. *Nanoscale Research Letters*, 10(1), p.490.
- [05] Khalid, A., Khan, I. and Shafie, S., 2015. Exact solutions for free convection flow of nanofluids with ramped wall temperature. *The European Physical Journal Plus*, 130(4), p.57.
- [06] Hamid, A., Hafeez, A., Khan, M., Alshomrani, A.S. and Alghamdi, M., 2019. Heat transport features of magnetic water-graphene oxide nanofluid flow with thermal radiation: Stability Test. *European Journal of Mechanics-B/Fluids*, 76, pp.434-441.
- [07] Cheng, P. and Minkowycz, W.J., 1977. Free convection about a vertical flat plate embedded in a porous medium with application to heat transfer from a dike. *Journal of Geophysical Research*, 82(14), pp.2040-2044.
- [08] Hong, J. T., Y. Yamada, and C. L. Tien. "Effects of non-Darcian and nonuniform porosity on vertical-plate natural convection in porous media." (1987): 356-362.
- [09] Lai, F.C. and Kulacki, F.A., 1991. Non-Darcy mixed convection along a vertical wall in a saturated porous medium. *Journal of Heat Transfer (Transactions of the ASME (American Society of Mechanical Engineers), Series C);(United States)*, 113(1).
- [10] Kandasamy, R., Muhaimin, I. and Rosmila, A.K., 2014. The performance evaluation of unsteady MHD non-Darcy nanofluid flow over a porous wedge due to renewable (solar) energy. *Renewable Energy*, 64, pp.1-9.
- [11] Sheikholeslami, M., Arabkoohsar, A. and Ismail, K.A.R., 2020. Entropy analysis for a nanofluid within a porous media with magnetic force impact using non-Darcy model. *International Communications in Heat and Mass Transfer*, 112, p.104488.

- [12] Ewis, K.M., 2020. A New Approach in Differential transformation method with application on MHD flow in non-Darcy medium between porous parallel plates considering hall current. *Advances in Water Resources*, 143, p.103677.
- [13] Von Karman T. Uber laminare und turbulente reibung. *Z Angew Math Mech*. 1921;1:233–52.
- [14] Millsaps K, Pohlhausen K. Heat transfer by laminar flow from a rotating plate. *J Aeronaut Sci*. 1952;19:120–6.
- [15] Fang T, Tao H. Unsteady viscous flow over a rotating stretchable disk with deceleration. *Commun Nonlinear Sci Numer Simul*. 2012;17(12):5064–72.
- [16] Turkyilmazoglu M, Uygun N. Basic compressible flow over a rotating disk. *Hacettepe J Math Stat*. 2004;33:1–10.
- [17] Miklavcic M, Wang CY. The flow due to a rough rotating disk. *Z Angew Math Phys*. 2004;55:235–46.
- [18] Turkyilmazoglu M. The MHD boundary layer flow due to a rough rotating disk. *Z Angew Math Mech*. 2010;90:72–82.
- [19] Turkyilmazoglu M. MHD fluid flow and heat transfer due to a stretching rotating disk. *Int J Therm Sci*. 2012;51:195–201.
- [20] Turkyilmazoglu M. Nanofluid flow and heat transfer due to a rotating disk. *Comput. Fluids*. 2014;94:139–46.
- [21] Griffiths PT. Flow of a generalized Newtonian fluid due to a rotating disk. *J Non-Newton Fluid Mech*. 2015;221:9–17.
- [22] Doh D H, Muthtamilselvan M. Thermophoretic particle deposition on magnetohydrodynamic flow of micropolar fluid due to a rotating disk. *Int J Mech Sci*. 2017;130:350.
- [23] Tabassum M, Mustafa M. A numerical treatment for partial slip flow and heat transfer of non-Newtonian Reiner-Rivlin fluid due to rotating disk. *Int J Heat Mass Transf*. 2018;123:979–87.
- [24] Appelquist E, Schlatter P, Alfredsson PH, Lingwood RJ. Turbulence in the rotating-disk boundary layer investigated through direct numerical simulations. *Eur J Mech-B/Fluids*. 2018;70:6–18.
- [25] Butt, A.S. and Ali, A., 2014. Entropy analysis of magnetohydrodynamic flow and heat transfer over a convectively heated radially stretching surface. *Journal of the Taiwan Institute of Chemical Engineers*, 45(4), pp.1197-1203.
- [26] Waini, I., Ishak, A. and Pop, I., 2019. Hybrid nanofluid flow induced by an exponentially shrinking sheet. *Chinese Journal of Physics*.
- [27] Naqvi, S.M.R.S., Muhammad, T., Saleem, S. and Kim, H.M., 2020. Significance of non-uniform heat generation/absorption in hydromagnetic flow of nanofluid due to stretching/shrinking disk. *Physica A: Statistical Mechanics and its Applications*, 553, p.123970.